

# Coke-resistant Pt-Ni/CeO<sub>2</sub>-SiO<sub>2</sub> Catalysts for Ethanol Reforming

Vincenzo Palma, Concetta Ruocco\*, Eugenio Meloni, Antonio Ricca

University of Salerno, D. I. In., Via Giovanni Paolo II 132, 84084 Fisciano (SA), Italy  
[ruocco@unisa.it](mailto:ruocco@unisa.it)

In this study, oxidative steam reforming of ethanol at low-temperature was investigated over bimetallic catalysts supported on CeO<sub>2</sub>/SiO<sub>2</sub>, having different ceria content (20–40 wt%). The activity was studied between 300 and 600°C, under a 10% C<sub>2</sub>H<sub>5</sub>OH/40% H<sub>2</sub>O/5% O<sub>2</sub>/45% N<sub>2</sub> stream; catalyst stability was evaluated at the same feeding conditions by fixing the temperature to 500°C. The results of catalyst characterization (BET, XRD, TPR) allowed the explanation of the different catalytic performances, in terms of activity and stability. The sample containing 30wt% of ceria displayed the highest durability, assuring total ethanol conversion and a stable behavior for more than 130 h. This result was related to the low dimension of Ni crystallites, which reduced carbon formation rate and improved catalyst resistance towards deactivation.

## 1. Introduction

Hydrogen, besides being a key reactant for petroleum and chemical industry, represents also an attractive energy source due to its high specific energy density, amplexness and eco-friendly nature (Oliveira et al., 2015). In fact, H<sub>2</sub> can be employed in fuel cells for electricity generation. Therefore, extensive researches have been made to develop efficient hydrogen production technologies. Currently, hydrogen is mainly produced from fossil fuels, such as natural gas and coal, via thermo-chemical processes. However, due to the environmental concerns and the limited availability of fossil fuels, bio-fuels (i.e. fuels derived from biomass sources that can be considered carbon neutral) provide an interesting sustainable solution (Nanda et al., 2016). Among these potential sources of H<sub>2</sub> generation, ethanol (C<sub>2</sub>H<sub>5</sub>OH), which is a renewable liquid fuel from biomass, is considered to be one of the ideal fuels for hydrogen. H<sub>2</sub> can be obtained from bio-ethanol by its steam reforming (SRE), partial oxidation (POE) or oxidative steam reforming (OSRE). However, bioethanol has certain advantages which encourage its use as raw material for reforming process: low toxicity, ease of handling and storage; in addition, only partial dehydration is required for crude bioethanol (water content ~86 wt%) in order to attain a steam/ethanol ratio suitable for steam reforming, thus avoiding the high cost of dehydration for ethanol use as fuel. Among the above technologies, steam reforming of ethanol is the most widely used method for H<sub>2</sub> production. However, due to the reaction endothermicity (173.27 KJ·mol<sup>-1</sup>), this process brings a relevant energy penalty (Palma et al., 2015 a). On the other hand, the high exothermicity of partial oxidation (-269.25 KJ·mol<sup>-1</sup>) could lead to hot-spots and catalyst deactivation. Therefore, oxidative steam reforming, which is performed by adding oxygen/air to the steam-ethanol feed at a rate able to guarantee auto-thermal conditions, has attracted increasing attention in recent years. In fact, the oxidative steam reforming of ethanol is more energy efficient as the reaction does not require an external heat supply. Oxygen co-feeding diminishes also the risk of carbon deposition on the surface and helps oxidize carbon already deposited on the surface in situ, regenerating the catalyst and resulting in catalyst activity sustaining for longer time. A wide range of catalysts, containing noble and non-noble metals as active species, was investigated for oxidative steam reforming of ethanol. In many cases, mixed oxides such as CeO<sub>2</sub>/ZrO<sub>2</sub> (Mondal et al., 2015), CeO<sub>2</sub>/Al<sub>2</sub>O<sub>3</sub>, CeO<sub>2</sub>/La<sub>2</sub>O<sub>3</sub> (Maia et al., 2014) were selected as support. Ceria, in fact, limits ethanol dehydration to ethylene (a well-known coke precursor), promotes water gas shift reaction and, due to its excellent oxygen mobility, promotes the gasification/oxidation of deposited carbon as soon it forms (Hou et al., 2014). Previous studies carried out by our research group (Palma et al., 2016) also displayed that the deposition of ceria on

mesoporous silica improve catalyst surface area and active species dispersion, resulting in better catalyst activity and stability.

The present work is focused on the study of CeO<sub>2</sub> loading effect on the activity and stability of bimetallic Pt-Ni/CeO<sub>2</sub>/SiO<sub>2</sub> catalysts for low-temperature oxidative steam reforming of ethanol (300-600°C).

## 2. Experimental

The bimetallic catalysts were prepared by sequential impregnation of CeO<sub>2</sub>, Ni and Pt on SiO<sub>2</sub> support. Silica gel (Aldrich) was preliminary calcined at 600°C (heating rate of 10°C/min) for 3 h. Ce(NO<sub>3</sub>)<sub>3</sub>·6H<sub>2</sub>O, Ni(NO<sub>3</sub>)<sub>2</sub>·6H<sub>2</sub>O and PtCl<sub>4</sub>, supplied by Strem Chemicals, were selected as CeO<sub>2</sub>, Ni and Pt salt precursors, respectively. After the addition of calcined silica to cerium nitrate aqueous solution, the solid was stirred, heated at 80 °C for 2 h on plate and finally separated by means of a Buchner funnel. Each impregnation was followed by sample drying overnight and calcination at the same conditions reported for SiO<sub>2</sub>. 10 wt% of Ni and 3 wt% of Pt were deposited on ceria by the same impregnation-drying-calcination procedure. Four samples were prepared at a CeO<sub>2</sub>/SiO<sub>2</sub> ratio of 20, 25, 30 and 40 wt%. The ceria-silica supports were identified as XCe while the symbol C-XCe was employed for the final catalysts.

The chemical composition of the supports and the Pt-Ni catalysts was investigated by X-ray fluorescence (XRF) spectrometry in a ThermoFischer QUANT'X EDXRF spectrometer equipped with a rhodium standard tube as the source of radiation. BET surface areas were measured by N<sub>2</sub> physisorption at its normal boiling point in a Sorptometer 1040 "Kelvin" from Costech Analytical Technologies. XRD patterns were registered on D-8 Advance Bruker WAXRD diffractometer ( $\lambda = 1.5406 \text{ \AA}$ ). The diffractograms of the fresh and spent catalysts were acquired between 20 and 80°. TPR (Temperature Programmed Reduction) measurements were carried out in the laboratory apparatus described below. Temperature was increased to 650 °C (heating rate of 10 °C·min<sup>-1</sup>) under a 5 %H<sub>2</sub> in N<sub>2</sub> stream; after the ramp, the sample was held at the maximum temperature for 1 h in the reducing atmosphere. The spent catalysts after stability tests were characterized by temperature programmed oxidation (TPO) from the temperature of the stability tests (500°C) to 600°C, with a rate of 3°C·min<sup>-1</sup>; the latter temperature was held until observing the closure of carbon oxides peaks, which gave a measurement of total carbon deposited on catalyst surface.

Activity and stability of C-XCe samples in the oxidative steam reforming of ethanol was evaluated in a fixed bed tubular stainless steel reactor having an annular configuration (i.d.=15 mm, o.d.=17 mm) under a continuous flow at atmospheric pressure. The reactor can be placed within an electrical oven and the allocation of catalytic bed, sandwiched within two quartz flakes, is selected in order to ensure a constant temperature in the catalytic layer. Prior to the reaction, 1.5 g of each catalyst sample was reduced in situ as described above. Nitrogen (131 Ncm<sup>3</sup>/min) was used as carrier gas during the reforming reaction. The results previously showed on the Pt-Ni/CeO<sub>2</sub>/SiO<sub>2</sub> system (Ruocco et al., 2016) suggests that CeO<sub>2</sub> forms a surface over-layer on SiO<sub>2</sub>, which is not directly involved in the catalytic process. Therefore, 1.5 g is the total mass of Pt+Ni+CeO<sub>2</sub> in the final catalyst. A liquid mixture of ethanol and bi-distilled water was continuously introduced in a boiler at a rate of 0.13 mL·min<sup>-1</sup> using a mass flow controller for liquids provided by Bronkhorst High-Tech; the mixture, having a molar ratio steam to ethanol (r.a.) fixed to 4, is stored in a tank under nitrogen pressure. The inlet and outlet lines of the reactor where heated at 130°C to maintain a vapor phase. The gas exiting the boiler was additionally mixed with air at the reactor entrance with an oxygen to ethanol molar ratio (r.o.) of 0.5. The reactants were fed to the reactor at a flow-rate of 500 Ncm<sup>3</sup>/min and the total ethanol feed rate with respect to catalyst weight (weight hourly space velocity, WHSV) was fixed to 4.1 h<sup>-1</sup>. The analysis of the reaction mixture and the reaction products (all in the gas phase) was carried out on-line by means of an FT-IR Spectrophotometer (Nicolet Antaris IGS by ThermoScientific). The hydrogen and oxygen concentrations were monitored by a thermoconductivity and a paramagnetic analyzer (supplied by ABB), respectively. In order to preserve normal ABB detectors, a cold trap was placed downstream the spectrophotometer. Activity tests were performed between 300 and 600°C and the performances of the C-XCe catalysts were evaluated in terms of ethanol conversion (Eq.1) and hydrogen yield (Eq.2). In order to evaluate the coking resistance of the investigated sample, the results of TPO measurements were employed for the calculation of carbon formation rate (CFR, Eq.3), defined as the ratio of total carbon deposited ( $m_{\text{coke}}$ ) on catalyst surface during the stability test and the product of catalytic mass ( $m_{\text{cat}}$ ), total mass of carbon fed as ethanol ( $m_{\text{carbon, fed}}$ ) and time-on-stream (TOS).

$$X = \frac{mol_{C_2H_5OH, in} - mol_{C_2H_5OH, out}}{mol_{C_2H_5OH, in}} \quad (1) \quad Y = \frac{mol_{H_2}}{6 * mol_{C_2H_5OH, in}} \quad (2)$$

$$CFR = \frac{m_{\text{coke}}}{m_{\text{carbon, fed}} m_{\text{cat}} * TOS} \quad (3)$$

### 3. Results and discussion

#### 3.1 Characterizations

It is well known that physiochemical properties of a catalyst play an important role in the evolution of the reaction. Table 1 lists the results of XRF and XRD analysis together with the BET surface area of the supports and the final catalysts. The chemical composition of the X-Ce and C-XCe sample was very close to the nominal values: the theoretical 3wt% of Pt and 10wt% of Ni, in fact, have to be calculated with respect to ceria content in the final catalyst. The supports and the catalysts containing 20 and 25 wt% of ceria displayed the highest specific surface area and a slight decrease in SSA value was observed with the growth in CeO<sub>2</sub> loading over both the series X-Ce and C-XCe. Moreover, the BET surface area of the support was not significantly affected by the addition of platinum and nickel.

Table 1: XRF, BET and XRD results.

Sample	SSA (m <sup>2</sup> /g)	CeO <sub>2</sub> wt%	Ni wt%	Pt wt%	d <sub>CeO<sub>2</sub></sub> (Å)	d <sub>NiO</sub> (Å)
20Ce	281	21.3	-	-	67	-
25Ce	294	24.8	2.22	0.60	64	-
30Ce	240	31.7	-	-	78	-
40Ce	242	41.9	-	-	78	-
C-20Ce	232	20.7	2.22	0.60	68	114
C-25Ce	239	23.8	2.93	0.97	62	135
C-30Ce	225	30.2	3.73	1.09	82	85
C-40Ce	219	39.4	4.8	1.25	73	127

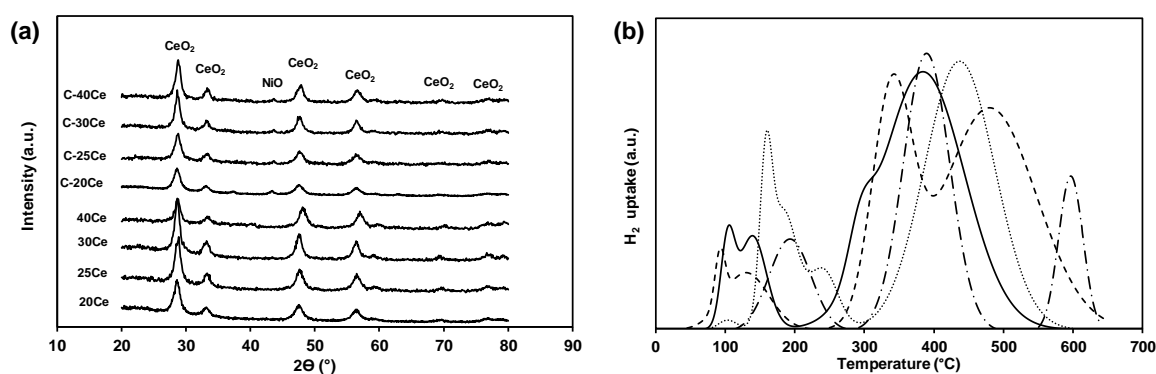


Figure 1: (a) XRD spectra and (b) deconvoluted TPR profile of the Pt-Ni/CeO<sub>2</sub>-SiO<sub>2</sub> catalysts (C-20Ce, point line segment; C-25Ce, dotted line; C-30Ce, continuous line; C-40Ce dashed line).

X-ray diffraction patterns of the bimetallic catalysts and the CeO<sub>2</sub>/SiO<sub>2</sub> supports having different ceria loadings were illustrated in Figure 1 (a). The diffraction patterns relative to CeO<sub>2</sub> fluorite structure were observed for all Ce-containing sample. Moreover, the CeO<sub>2</sub> characteristic lines were not shifted to higher 2 $\theta$  values, which indicated that ceria was not incorporated into silica structure (Reddy et al., 2009). In fact, since the specific area of the used mesoporous silica is very large, the CeO<sub>2</sub> particles are highly dispersed on the surface of SiO<sub>2</sub>, thus avoiding the formation of lattice structures. The presence of the amorphous phase is indicated by a broad hump in the X-ray diffraction spectrum over a range of 2 $\theta$  angles (Amin et al., 2016). It can also be seen that peaks at 2 $\theta$  = 43.9° for all the catalysts originate from characteristic diffraction of crystalline nickel oxide; conversely, the high dispersed Pt oxides species were not identified in Figure 1 (a). The average crystallite sizes of CeO<sub>2</sub> and NiO particles are presented in Table 1. The dimension of ceria crystallites ranged from 6 to 8 nm, highlighting a negligible effect of both ceria loading and active species deposition on CeO<sub>2</sub> dispersion. On the other hand, the sizes of NiO particles changed in a wider range and the lowest dimension (85 Å) was measured over the C-30Ce catalyst. Figure 1 (b) compares the hydrogen consumption profiles of the C-XCe catalysts acquired during TPR measurements, which were performed to investigate the redox characteristics. The TPR profiles can be divided into three temperature regions: region I (50-200°C), region II (200-400°C) and region III (400-650°C). The low-temperature peaks can be assigned to the reduction of PtO<sub>x</sub> particles, interacting with Ni and/or with the support, able to promote a surface ceria reduction as well as a beforehand NiO reduction due to the hydrogen spillover effects (Palma et al., 2012). Region II can be correlated to the reduction of free NiO and nickel oxide particles having a significant interaction with the

support. At  $T > 400^\circ\text{C}$ , it is possible to observe the surface and bulk reduction of ceria (Peng et al., 2016), enhanced by Platinum and Nickel. Moreover, it was shown (Mamontov et al., 2016) that the combination of ceria and silica can result in an increased oxygen storage capacity in comparison with the one observed with  $\text{CeO}_2$  and  $\text{SiO}_2$  alone. As a result, for all the catalysts, the total hydrogen consumption was higher (3608, 3712, 3802 and  $4790 \mu\text{mol/g}_{\text{cat}}$  for C-20Ce, C-25Ce, C-30Ce and C-40Ce, respectively) than that expected for complete  $\text{NiO}$  and  $\text{PtO}_x$  reduction ( $2012 \mu\text{mol/g}_{\text{cat}}$ ). In addition, the catalyst reducibility (and in particular the reduction of  $\text{PtO}_x$  particles, which was subjected to a leftward shift peak) was promoted by the growth in ceria loading from 20 to 40 wt%.

### 3.2 Catalytic performances for oxidative steam reforming of ethanol

Catalytic performances of the C-XCe series for oxidative steam reforming of ethanol in the temperature interval of  $300\text{--}600^\circ\text{C}$  are shown in Figure 2 (a) and (b). The catalytic activity was evaluated in terms of ethanol conversion and hydrogen yield at  $\text{H}_2\text{O}/\text{C}_2\text{H}_5\text{OH}$  and  $\text{O}_2/\text{C}_2\text{H}_5\text{OH}$  ratio of 4 and 0.5, respectively. The average values of ethanol conversion as a function of reaction temperature highlighted interesting catalytic performances for all the samples. In fact, total conversion was measured until  $350^\circ\text{C}$  over the Pt-Ni/ $\text{CeO}_2/\text{SiO}_2$  catalysts. For lower temperatures, decreased activity was observed, especially over the C-20 and C-25 samples, which displayed ethanol conversion equal or lower than 60% at  $300^\circ\text{C}$ . On the other hand, the catalyst containing 30wt% of ceria assured total ethanol conversion even at  $320^\circ\text{C}$ , reaching a 90% of conversion at  $300^\circ\text{C}$ .

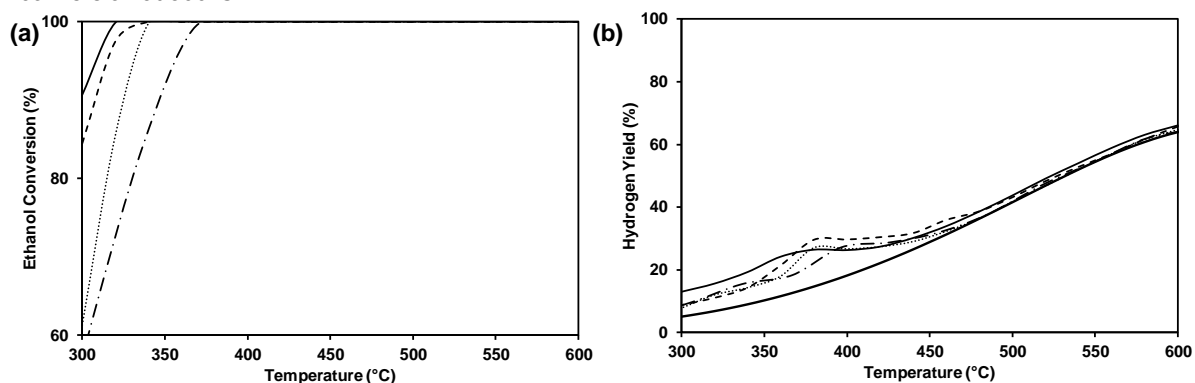


Figure 2: (a) Ethanol conversion and (b) hydrogen yield recorded over the Pt-Ni/ $\text{CeO}_2\text{-SiO}_2$  catalysts (C-20Ce, point line segment; C-25Ce, dotted line; C-30Ce, continuous line; C-40Ce dashed line, equilibrium thick line);  $r.a.=4$ ,  $r.o.=0.5$ ;  $\text{WHSV}=4.1 \text{ h}^{-1}$ .

Hydrogen yield was very close to the values predicted by thermodynamic equilibrium in the high temperature interval: an average increase from 38 to 64% was observed with a temperature variation between 500 and  $600^\circ\text{C}$ . For  $T < 450^\circ\text{C}$ , it was found that the experimental yields were higher than the expected values over all the C-XCe catalysts. Such phenomenon, previously discussed (Palma et al., 2015 b), can be explained looking at the complex kinetics of the reaction, which hindered the system in reaching thermodynamic predictions. In order to reveal the catalysts resistance towards deactivation, long-term stability tests were performed at an intermediate temperature ( $500^\circ\text{C}$ ), observing a strong effect of  $\text{CeO}_2/\text{SiO}_2$  ratio on carbon formation rate. All the bimetallic catalysts assured very high durability and total ethanol conversion was measured for at least 50 h Figure 3 (a)). Moreover, the products mixture only contained  $\text{H}_2$ ,  $\text{H}_2\text{O}$ ,  $\text{C}_2\text{H}_5\text{OH}$  (eventually),  $\text{CH}_4$ ,  $\text{CO}$  and  $\text{CO}_2$  while other by-products (i.e. acetone, acetaldehyde and ethylene) were not detected. This result appeared very interesting when compared with the recent literature studies (Morales et al., 2015; Mondal et al., 2015; Jin et al., 2016). In fact, oxidative steam reforming of ethanol, at space velocity similar to that selected in the present work, was rarely carried out for so many hours and the product gas distribution often displayed a very fast deactivation. The impressive performances of the Pt-Ni/ $\text{CeO}_2/\text{SiO}_2$  series can be explained looking at the results of physicochemical characterization. The C-XCe sample displayed very high ( $> 200 \text{ m}^2/\text{g}$ ) specific surface areas, which reduced the dimension of ceria and metal particle sizes. As a result, the better interaction between the active species and the support may improve catalyst activity and limit coke formation (Zhao et al., 2016). Moreover, the choice of a  $\text{CeO}_2/\text{SiO}_2$  mixed oxide as catalytic support further enhanced the oxygen storage and transfer capacity of ceria, due to the increased number of oxygen vacancies, thus promoting the oxidation of carbonaceous species deposited on catalyst surface (Rotaru et al., 2015). According to the results obtained in terms of catalyst activity, the most pronounced increase in ethanol concentration was recorded over the catalyst containing 20 wt% of ceria, which displayed a conversion of 92% after 70 h of time-on-stream. The ceria content growth between 20 and

30% strongly improved the catalytic resistance towards deactivation and, as a result, the C-25Ce sample showed total ethanol conversion for almost 100 h. Moreover, the sample prepared at a  $\text{CeO}_2/\text{SiO}_2$  ratio of 30 reached the highest performances in terms of durability: complete conversion was measured for more than 135 h and conversion was only lowered to 99% after 145 h of reaction. However, a further increase in ceria loading (between 30 and 40 wt%), differently from the forecasts suggested by the above results, reduced the stability performances of the C-30Ce catalyst. In fact, despite the two catalyst having the highest ceria content assured total ethanol conversion for almost the same hours, a faster increase of ethanol concentration was recorded over the C-40Ce sample, which after 135 h, reached a  $\text{C}_2\text{H}_5\text{OH}$  conversion of 92%.

After stability tests, oxidation measurements were carried out to evaluate the different carbon formation rates of the four catalysts. Moreover, the CFR was related to the average size of nickel crystallites ( $d_{\text{Ni}}$ ), determined through X-ray diffraction analysis on the spent catalysts, and the results are shown in Figure 3 (b).

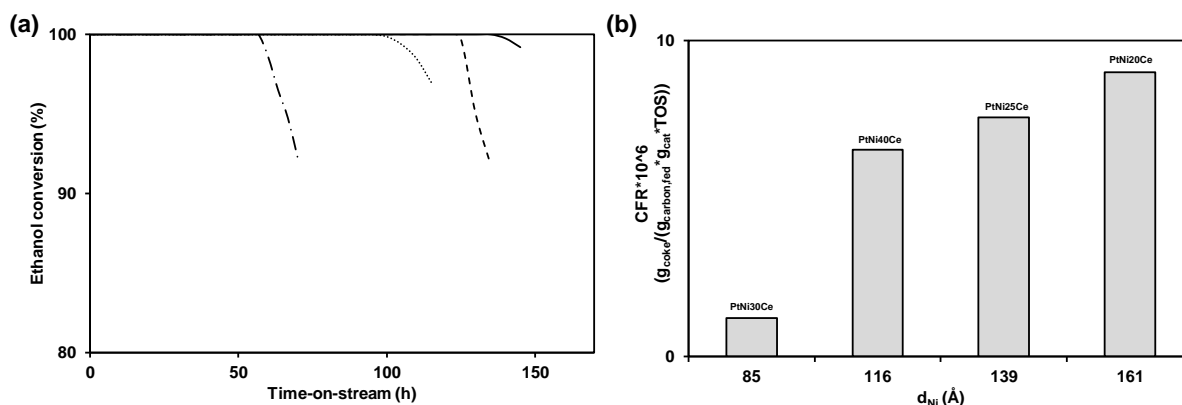


Figure 3: (a) Ethanol conversion as a function of TOS ( $T=450^\circ\text{C}$ ,  $r.a.=4$ ,  $r.o.=0.5$ ,  $\text{WHSV}=4.1 \text{ h}^{-1}$ , C-20Ce, point line segment; C-25Ce, dotted line; C-30Ce, continuous line; C-40Ce dashed line) and (b) relationship between CFR and average crystallite sizes of Ni particles.

First of all, it's interesting to observe that all the catalysts of the C-XCe series displayed very low carbon formation rates (of the order of  $10^{-6} \text{ g}_{\text{coke}}/(\text{g}_{\text{carbon, fed}} \cdot \text{g}_{\text{cat}} \cdot \text{TOS})$ ). Conversely other authors (da Silva et al. 2011; de Lima et al. 2012) despite selected less stressful operative conditions (i.e. lower ethanol concentration in the reacting mixture, a key parameter which affects coke selectivity) than that fixed in the present work, measured higher carbon formation rates. The reduction of ceria loading from 25 to 20 wt% worsened the carbon formation rate, which increased from 7.6 to  $9 \cdot 10^{-6} \text{ g}_{\text{coke}}/(\text{g}_{\text{carbon, fed}} \cdot \text{g}_{\text{cat}} \cdot \text{TOS})$ . In addition, the results of XRD analysis proved that a lower  $\text{CeO}_2/\text{SiO}_2$  ratio negatively affected Ni particle sizes, which increased from 139 to 161 Å. The best results, in terms of both carbon formation rate and  $d_{\text{Ni}}$  (equal, respectively, to  $1.2 \cdot 10^{-6} \text{ g}_{\text{coke}}/(\text{g}_{\text{carbon, fed}} \cdot \text{g}_{\text{cat}} \cdot \text{TOS})$  and 85 Å) were observed over the C-X30Ce sample, which also displayed the highest activity and stability for oxidative steam reforming of ethanol. However, the growth in ceria loading from 30 to 40 wt% was not accompanied by the desired improvement of active species dispersion and a CFR almost 5 times higher than that observed over the C-X30Ce catalyst was measured. A strong correlation, in fact, exist between the average crystallite size of Ni particles and the carbon formation tendency of the catalyst (Vizcaíno et al., 2007): the smallest Ni crystallites may assure the lower carbon deposition. In fact, when the available surface area of nickel particles is high, the residence time of coke precursors may increase, thus offering an easy route for more stable carbonaceous deposits formation.

#### 4. Conclusions

The present work is focused on the preparation, characterization and performances evaluation for oxidative steam reforming of ethanol of a series of Pt-Ni/ $\text{CeO}_2/\text{SiO}_2$  catalysts, having a ceria/silica ratio in the range 20-40 wt%. All the samples displayed high specific surface area, good dispersion of nickel oxide and relevant redox properties. A preliminary activity screening, carried out between 300 and 600°C, at a  $r.a.=4$ ,  $r.o.=0.5$  and  $\text{WHSV}=4.1 \text{ h}^{-1}$ , revealed that all the catalyst can assure total ethanol conversion at  $T > 360^\circ\text{C}$ . On the other hand, an improving in low-temperature activity was observed by increasing  $\text{CeO}_2/\text{SiO}_2$  ratio from 20 to 30 wt%. However, a further growth in ceria content had no positive effect on ethanol conversion. The long-term stability of the four catalysts was investigated at 500°C for at least 70 h. The catalyst resistance towards deactivation increased in the following order: C-30Ce > C-40Ce > C-25Ce > C-20Ce: the catalyst containing the 30wt% of ceria displayed total ethanol conversion for almost 135 h and the lowest carbon formation rate ( $1.2 \cdot 10^{-6} \text{ g}_{\text{coke}}/(\text{g}_{\text{carbon, fed}} \cdot \text{g}_{\text{cat}} \cdot \text{TOS})$ ). The average crystallite sizes of Ni particles for the spent catalysts was

measured, finding that the increase of CeO<sub>2</sub>/SiO<sub>2</sub> ratio can improve Ni dispersion and the maximum in the performances can be obtained for a ceria loading equal to 30 wt%.

### Acknowledgments

The research leading to these results has received funding from the European Union's Seventh Framework Programme (FP7/2007-2013) for the Fuel Cells and Hydrogen Joint Technology Initiative under grant agreement n° 621196. Note: "The present publication reflects only the authors' views and the FCH JU and the Union are not liable for any use that may be made of the information contained therein".

### References

- Amin N., Khattak S., Noor S., Ferroze I., 2016, Synthesis and characterization of silica from bottom ash of sugar Industry, *Journal of Cleaner Production*, 117, 206-211.
- da Silva A., de Souza K., Mattos L., Jacobs G., Davis B., Noronha F., 2011, The effect of support reducibility on the stability of Co/CeO<sub>2</sub> for the oxidative steam reforming of ethanol, *Catalysis Today*, 164, 234-239.
- de Lima S., da Silva A., Assaf J., Mattos L., Noronha F., 2012, Hydrogen production through OESR over Ni-based catalysts derived from La<sub>1-x</sub>Ce<sub>x</sub>NiO<sub>3</sub> perovskite-type oxides, *Applied Catalysis B: Environmental* 121-122, 1-9.
- Hou T., Zhang S., Xu T., Cai W., 2014, Hydrogen production from oxidative steam reforming of ethanol over Ir/CeO<sub>2</sub> catalysts in a micro-channel reactor, *Chemical Engineering Journal*, 255 149-155.
- Jin Y., Rui Z., Tian Y., Y.S. Lin Y.S.; Li Y., 2016, Autothermal reforming of ethanol in dense oxygen permeation membrane reactor, *Catalysis Today*, 264, 214-220.
- Maia T., Assaf J., Assaf E., 2014, Study of Co/CeO<sub>2</sub>- $\gamma$ -Al<sub>2</sub>O<sub>3</sub> catalysts for steam and oxidative reforming of ethanol for hydrogen production, *Fuel Processing Technology*, 18, 134-145.
- Mamontov G.V., Grabchenko M.V., Sobolev V.I., Zaikovskii V.I., O.V. Vodyankina O.V., 2016, Ethanol dehydrogenation over Ag-CeO<sub>2</sub>/SiO<sub>2</sub> catalyst: Role of Ag-CeO<sub>2</sub> interface, *Applied Catalysis: A General*, 528, 161-167.
- Mondal T., Pant K., Dalai A., 2015, Oxidative and non-oxidative steam reforming of crude bio-ethanol for hydrogen production over Rh promoted Ni/CeO<sub>2</sub>-ZrO<sub>2</sub> catalyst, *Applied Catalysis A: General*, 499, 19-31.
- Morales M. and Segarra M., 2015, Steam reforming and oxidative steam reforming of ethanol over La<sub>0.6</sub>Sr<sub>0.4</sub>CoO<sub>3- $\delta$</sub>  perovskite as catalyst precursor for hydrogen production, *Applied Catalysis A: General*, 502, 305-311.
- Nanda S., Casalino M., Loungia M.S., Dalai A.K., Gökalp I., A. Kozinski J.A., 2016, Catalytic Gasification of Pinewood in Hydrothermal Conditions for Hydrogen Production, *Chemical Engineering Transactions*, 50, 31-36.
- Oliveira F., Araujo A., Romão B., Cardoso V., Ferreira J., Batista F., 2015, Hydrogen Photo Production using *Chlorella* sp. through Sulfur-deprived and Hybrid System Strategy, *Chemical Engineering Transactions*, 43, 301-306.
- Palma V., Castaldo F., Ciambelli P., Iaquaniello G., 2012, Hydrogen production through catalytic low-temperature bio-ethanol steam reforming, *Clean Technologies and Environmental Policy*, 14, 973-987.
- Palma V., Ruocco C., Castaldo F., Ricca A., Boettge D., 2015b, Ethanol steam reforming over bimetallic coated ceramic foams: Effect of reactor configuration and catalytic support, *International Journal of Hydrogen Energy*, 40 12650-62.
- Palma V., Ruocco C., Meloni M., Ricca A., 2016, Activity and Stability of Novel Silica-Based Catalysts for Hydrogen Production via Oxidative Steam Reforming of Ethanol, *Chemical Engineering Transactions*, 52, 67-72.
- Palma V., Ruocco C., Ricca A., 2015a, Bimetallic Pt and Ni Based Foam Catalysts for Low-Temperature Ethanol Steam Reforming Intensification, *Chemical Engineering Transactions*, 43, 559-564.
- Peng R., Sun X., Li S., Chen L., Fu M., Wu J., Ye D., 2016, Shape effect of Pt/CeO<sub>2</sub> catalysts on the catalytic oxidation of toluene, *Chemical Engineering Journal*, 306, 1234-1246.
- Reddy B.M., Saikia P., Bharali P., Katta L., Thrimurthulu G., 2009, Highly dispersed ceria and ceria-zirconia nanocomposites over silica surface for catalytic applications, *Catalysis Today*, 141, 109-114.
- Rotaru C.G., Postole G., Florea M., Matei-Rutkovska F., Pârvulescu V., Gelin P., 2015, Dry reforming of methane on ceria prepared by modified precipitation route, *Applied Catalysis A : General*, 494, 29-40.
- Ruocco C., Meloni E., Palma V., Van Sint Annaland M., Spallina V., Gallucci F., 2016, Pt-Ni based catalyst for ethanol reforming in a fluidized bed membrane reactor, *International Journal of Hydrogen Energy*, 41, 20122-20136.
- Vizcaino A.J., Carrero A., J.A. Calles J.A., 2007, Hydrogen production by ethanol steam reforming over Cu-Ni supported catalysts, *International Journal of Hydrogen Energy*, 32, 1450-1461.